Numerical Methods in Civil Engineering, 10-4 (2026) 44-58

**Numerical Methods in Civil Engineering**

Journal Homepage: https://nmce.kntu.ac.ir/

# The effect of wind intensity on the optimal location of outriggers for minimizing base moment and maximum building displacement

**Sajjad Baygi*, Amin Khazaee****

*ARTICLE INFO*

RESEARCH PAPER

*Article history:*
*Received:*
*June 2026*
*Revised:*
*August 2026*
*Accepted:*
*September 2026*

*Keywords:*
*Outrigger;*
*Optimal location;*
*Wind Load;*
*Base moment;*
*Maximum displacement*

**Abstract:**

This study investigates the influence of wind load intensity on the optimal location of outrigger systems in high-rise buildings, aiming to minimize the base moment and the maximum lateral displacement. The proposed analytical model assumes uniform material properties throughout the building height and identical flexural rigidity for all outrigger levels. Analyses are conducted for four wind load intensities and structural configurations incorporating one to four outriggers. The governing mathematical formulations are derived and implemented through MATLAB-based numerical procedures to determine the optimal outrigger locations. The results demonstrate that increasing wind load intensity shifts the optimal outrigger positions toward higher elevations of the structure while reducing the vertical spacing between them. Furthermore, an increase in the flexural rigidity of the central core or a reduction in the flexural rigidity of the outriggers leads to a similar upward shift in the optimal locations. It is also shown that the optimal outrigger location for minimizing the base moment occurs at lower elevations compared to that required to minimize the maximum lateral displacement.

## 1. Introduction

In recent years, high-rise buildings have been widely constructed and continue to play a crucial role in meeting the growing demands of urban development. Owing to their importance in modern cities, tall buildings have become a fundamental component of urban infrastructure worldwide [1–3]. Rapid advancements in construction technologies, building materials, and sophisticated structural analysis and design methods supported by computer-based tools have further facilitated the proliferation of high-rise buildings, particularly in countries with emerging economies. Due to their relatively low inherent damping and long fundamental natural periods, high-rise buildings are especially sensitive to wind-induced loads. These characteristics may result in large- amplitude wind- induced vibrations, which can significantly affect both structural safety and occupant comfort [4].

** Corresponding Author: Assistant Professor, Department of Civil Engineering, Esfarayen University of Technology, Esfarayen, Iran. https://orcid.org/0000-0003-1480-9268; Email:s.baygi@esfarayen.ac.ir*
*** Assistant Professor, Department of Civil Engineering, Esfarayen University of Technology, Esfarayen, Iran. https://orcid.org/0009-0007-8688-6306; Email:a.khazaie@esfarayen.ac.ir*

Consequently, the selection and implementation of efficient lateral load-resisting systems are essential to control lateral displacements and internal force demands in tall structures. Among various lateral load-resisting systems, outrigger and belt truss systems are recognized as one of the most effective and commonly adopted solutions for tall and super-tall buildings [5]. These systems function as cantilever-type structural components that extend from the central core to the perimeter columns, forming an integrated structural framework [6]. By redistributing lateral forces and enhancing global lateral stiffness, outrigger systems substantially reduce lateral displacements and improve the overall structural performance under lateral loading conditions [7]. Despite their widespread application, determining the optimal placement of outrigger systems remains a significant challenge in the structural design of high-rise buildings [8]. By acting as a large structural frame composed of the central core, perimeter columns, and outrigger trusses, the outrigger system enhances lateral stiffness and reduces lateral displacements and bending moments in the core under to wind or seismic loading [9,10]. Furthermore, belt truss systems connect the exterior columns

https://doi.org/10.66224/NMCE.2606.1146

to the central core, enabling both components to resist core rotation, which in turn reduces overall structural drift and base moment in the core [11–13]. This study proposes a comprehensive analytical framework to investigate the influence of wind load intensity on the optimal placement of outrigger systems in high-rise buildings. Unlike previous studies that primarily focused on uniform lateral loads or relied on simplified assumptions, the present research systematically examines the effect of varying wind load intensities on the optimal outrigger locations with two distinct objectives: minimizing the maximum lateral displacement and minimizing the base moment of the central core. By deriving analytical formulations and implementing them within a numerical algorithm, this study provides quantitative results that can be directly applied in engineering design. The findings offer practical insights for optimizing outrigger systems in tall buildings subjected to wind loading. Numerous studies have been conducted to optimize the performance of outrigger systems in high-rise buildings. Xing et al. employed the pseudo-excitation method to investigate optimal outrigger locations and optimal damping parameters for combined energy-dissipating outrigger systems subjected to wind and seismic loads [14]. Smith and Coull analyzed the optimal outrigger locations for minimizing the maximum lateral displacement in structures equipped with one to four outriggers [10]. Kim et al. determined the optimal placement of outriggers aimed at minimizing top-story lateral displacement in tall buildings using a gradient-based nonlinear programming approach [15]. Taranath investigated optimal outrigger locations using a simplified structural model in which the outriggers were assumed to be infinitely rigid; however, the study also highlighted that outrigger stiffness significantly affects global drift, core moment, and the optimal outrigger location for maximum drift reduction [16]. Lee and Tovar proposed a topology-optimization-based design method for determining the placement of outrigger systems in tall buildings, assuming rigid outriggers [17]. Kamgar and Rahgozar introduced an approach for identifying the optimal location of flexible outrigger systems based on maximizing the strain energy of belt truss–outrigger systems [18]. Additionally, Hoenderkamp et al. [19] analyzed outrigger systems in various structural configurations by incorporating the shear stiffness of braced frames and outriggers through modified analytical formulations. Wu and Li [20] investigated the optimal design of tall buildings with multiple outriggers by analyzing the effects of outrigger locations and structural stiffness on the upper drift and fundamental vibration period under uniform and triangular lateral loads. More recently, Afshar et al. [21] proposed several alternative configurations for damped outrigger systems and examined their dynamic performance through time- and frequency-domain analyses, focusing on vibration control and optimal damping parameters. Although these studies significantly advanced the understanding of outrigger behavior, they primarily addressed the optimization of outrigger configurations for given loading conditions or dynamic vibration control problems. A systematic analytical investigation of how variations in wind loading intensity influence the optimal outrigger locations corresponding to different structural performance objectives has received limited attention. The present study addresses this gap by developing closed-form analytical relationships that quantify the influence of wind loading intensity on the optimal placement of conventional outrigger systems for minimizing both the core base moment and the maximum lateral displacement.

The present study evaluates the two structural performance objectives independently in order to clearly distinguish the influence of wind loading intensity on each response criterion. Although this approach provides valuable insight into the underlying structural mechanics, practical structural design generally requires a balance between multiple performance objectives. The analytical relationships developed in this study can therefore serve as efficient objective functions within future multi-objective optimization frameworks, such as Pareto-based optimization, to identify compromise outrigger configurations that simultaneously reduce both the base moment and the maximum lateral displacement.

## 2. Analytical Formulation

Although the present study focuses exclusively on equivalent static wind loading, practical design of tall buildings frequently requires consideration of both wind and seismic actions. Unlike wind loading, which is characterized by externally applied lateral forces with a prescribed lateral distribution, seismic loading generates inertia forces that depend on the mass distribution, vibration modes, and dynamic characteristics of the structure. Consequently, the optimal outrigger locations obtained under wind loading may differ from those corresponding to seismic excitation. Therefore, the analytical framework developed in this study may be extended in future research to investigate the influence of seismic loading or combined wind–earthquake loading on the optimal placement of outrigger systems. Such an extension would provide a more comprehensive basis for performance-based design of tall buildings.

In this study, high-rise buildings equipped with outrigger systems are modeled as a central core connected to perimeter columns through outriggers and belt trusses. Due to the high number of structural parameters involved in analyzing such systems, the following simplifying assumptions are considered [10]:

1. The structural behavior is assumed to be linearly elastic.

2. Shear forces in the columns are neglected.
3. The outrigger-to-core connection is assumed rigid, while the outrigger-to-column connection is considered pinned.
4. The flexural rigidity of the structural core, perimeter columns, and outrigger elements is assumed to remain constant over the entire building height.

The present analytical formulation is based on the assumption of linear elastic structural behavior and therefore does not explicitly account for second-order geometric (P–Δ) effects. This assumption was adopted to enable the derivation of closed-form analytical relationships and to facilitate a clear investigation of the influence of wind loading intensity on the optimal placement of outrigger systems. Although P–Δ effects may become significant in very slender or super-tall buildings subjected to severe lateral loading, the proposed model is primarily intended for preliminary design applications and analytical assessment within the elastic range. Future studies may extend the present formulation by incorporating geometric nonlinearity to evaluate its influence on the optimal outrigger configuration.

The proposed analytical formulation neglects the contribution of shear lag in the perimeter columns, consistent with the assumptions adopted in many classical closed-form analytical models of outrigger systems. This simplification facilitates the derivation of explicit analytical relationships and enables a clear assessment of the influence of wind loading intensity on the optimal placement of outriggers. Nevertheless, shear lag may affect the distribution of axial forces and bending moments in perimeter columns, particularly in slender buildings with complex belt truss configurations.

### *1.1 Structure with Two Outriggers*

To derive the governing analytical relations, a structure with two outriggers is initially considered, and the resulting equations are later generalized for a system with (n) outriggers.

The equivalent static wind load acting along the height of the building is assumed to follow the following distribution:

$$q(x) = w(H - x)^{\beta} \quad (1)$$

Where q(x) is the lateral wind load intensity at elevation x, w is the reference wind load intensity, H is the total height of the structure, and β is the wind load distribution coefficient controlling the variation of the wind load along the building height. Higher values of β represent a greater concentration of the wind load toward the upper portion of the structure. The adopted wind load profile is illustrated schematically in Figure 1. The bending moment diagram and its equation for the central core in the absence of the outrigger, derived using equilibrium equations, are shown in Figure 1.

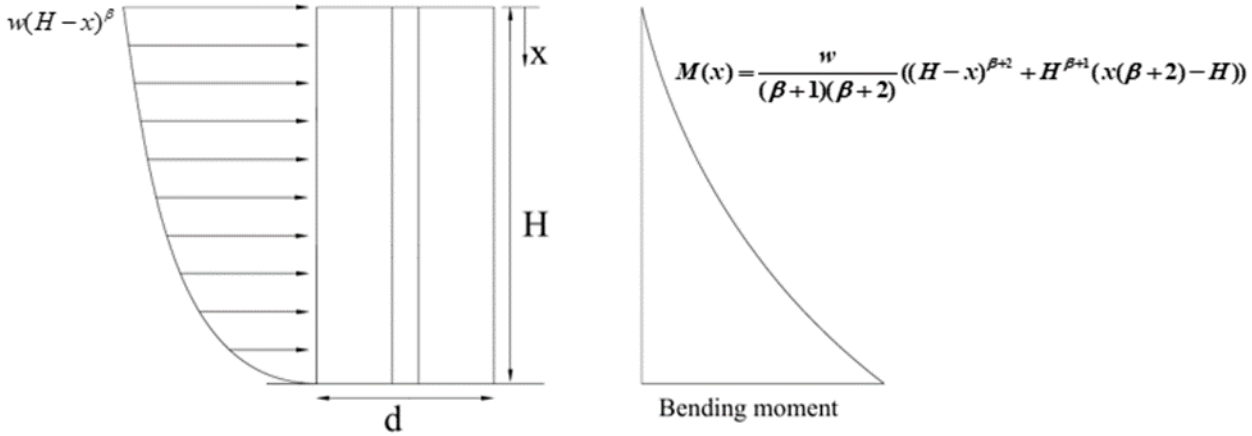


**Fig. 1:** Bending moment induce in the central core under wind load

The presence of outriggers significantly reduces both lateral displacements and bending moments in the central core. The magnitude of moment reduction depends on the mechanical properties of the core, perimeter columns, and the flexural stiffness of the outriggers. Denoting the moment reduction provided by an outrigger at elevation x1 as M1 and at x2 as M2, the resulting moment distributions with and without outriggers are depicted in Figure 2.

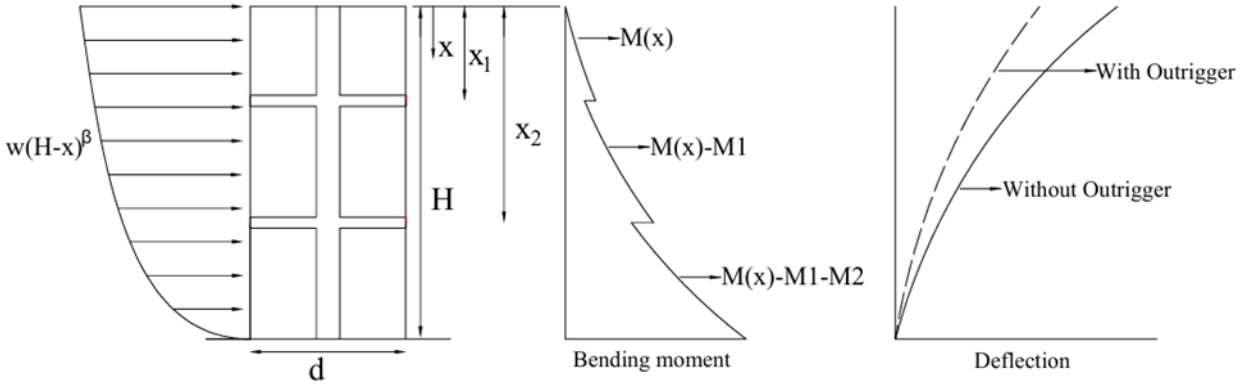


**Figure. 2.** Moment and displacement generated in a building with two outriggers.

For a structure with two outriggers, the core rotations at levels x1 and x2 due to core bending are obtained from Eq. (1).

$$\theta_1 = \frac{1}{EI}\int_{x_1}^{x_2}((\frac{w}{(\beta+1)(\beta+2)}(H-x)^{\beta+2} + \\ +H^{\beta+1}(x(\beta+2)-H)) - M_1))dx \\ +\frac{1}{EI}\int_{x_2}^{H}(\frac{w}{(\beta+1)(\beta+2)}(H-x)^{\beta+2} + \\ H^{\beta+1}(x(\beta+2)-H)) - M_1 - M_2)dx \\ \theta_2 = \frac{1}{EI}\int_{x_2}^{H}((\frac{w}{(\beta+1)(\beta+2)}(H-x)^{\beta+2} \\ H^{\beta+1}(x(\beta+2)-H)) - M_1 - M_2)dx \quad (1)$$

Where (EI) represents the flexural rigidity of the central core, and (Θ1) and (Θ2) denote the rotations at elevations x1 and x2, respectively.

Due to axial forces in the columns and bending in the outriggers, additional rotations occur at the outrigger–core connections. Considering these effects, the rotations at x1 and x2 are expressed in Eqs. (3) and (4),

$$\theta_1 = \frac{2M_1(H-x_1)}{d^2(EA)_C} + \frac{2M_2(H-x_2)}{d^2(EA)_C} + \frac{M_1 d}{12(EI)_o} \quad (3)$$

$$\theta_2 = \frac{2(M_1+M_2)(H-x_1)}{d^2(EA)_C} + \frac{M_2 d}{12(EI)_o} \quad (4)$$

Where $(EA)_C$ and $(EI)_o$ are the axial stiffness of the columns and the flexural stiffness of the outriggers, respectively.

By enforcing rotational compatibility, the rotations of the outrigger and the core at the connection points must be equal. Accordingly, the compatibility relations at levels x1 and x2 are given in Eqs. (5) and (6).

$$\frac{1}{EI}\int_{x_1}^{x_2}((\frac{w}{(\beta+1)(\beta+2)}(H-x)^{\beta+2} + \\ +H^{\beta+1}(x(\beta+2)-H)) - M_1))dx \\ +\frac{1}{EI}\int_{x_2}^{H}(\frac{w}{(\beta+1)(\beta+2)}(H-x)^{\beta+2} + \\ H^{\beta+1}(x(\beta+2)-H)) - M_1 - M_2)dx = \\ \frac{2M_1(H-x_1)}{d^2(EA)_C} + \frac{2M_2(H-x_2)}{d^2(EA)_C} + \frac{M_1 d}{12(EI)_o} \quad (5)$$

$$\frac{1}{EI}\int_{x_2}^{H}((\frac{w}{(\beta+1)(\beta+2)}(H-x)^{\beta+2} \\ H^{\beta+1}(x(\beta+2)-H)) - M_1 - M_2)dx = \\ \frac{2(M_1+M_2)(H-x_2)}{d^2(EA)_C} + \frac{M_2 d}{12(EI)_o} \quad (6)$$

After algebraic simplification, the final governing relations are expressed in Eqs. (7) and (8).

$$M_1\left[S_1 + S(H-x_1)\right] + M_2\left[S(H-x_2)\right] = \frac{w}{EI} \\ \left(\frac{2(H-x_1)^{\beta+3} + (\beta+3)(H-x_1)H^{\beta+1}(\beta(H+x_1)+2x_1)}{2(\beta+1)(\beta+2)(\beta+3)}\right) \quad (7)$$

$$M_1\left[S(H-x_2)\right] + M_2\left[S_1 + S(H-x_2)\right] = \frac{w}{EI} \\ \left(\frac{2(H-x_2)^{\beta+3} + (\beta+3)(H-x_2)H^{\beta+1}(\beta(H+x_2)+2x_2)}{2(\beta+1)(\beta+2)(\beta+3)}\right) \quad (8)$$

$$S = \frac{1}{EI} + \frac{2}{d^2(EA)_C}\ , S_1 = \frac{d}{12(EI)_o} \quad (9)$$

By expressing Eqs. (7) and (8) in matrix form, Eq. (10) is obtained, enabling the calculation of the restraint moments at x1 and x2. Subsequently, the outrigger moments are determined from Eq. (11).

$$\begin{bmatrix} S_1 + S(H-x_1) & S(H-x_2) \\ S(H-x_2) & S_1 + S(H-x_2) \end{bmatrix}\begin{bmatrix} M_1 \\ M_2 \end{bmatrix} = \frac{w}{EI} \\ \begin{bmatrix} \frac{2(H-x_1)^{\beta+3} + (\beta+3)(H-x_1)H^{\beta+1}(\beta(H+x_1)+2x_1)}{2(\beta+1)(\beta+2)(\beta+3)} \\ \frac{2(H-x_2)^{\beta+3} + (\beta+3)(H-x_2)H^{\beta+1}(\beta(H+x_2)+2x_2)}{2(\beta+1)(\beta+2)(\beta+3)} \end{bmatrix} \quad (10)$$

$$\begin{bmatrix} M_1 \\ M_2 \end{bmatrix} = \frac{w}{EI} A_1^{-1} B_1$$

$$A_1 = \begin{bmatrix} S_1 + S(H - x_1) & S(H - x_2) \\ S(H - x_2) & S_1 + S(H - x_2) \end{bmatrix}$$

$$B_1 = \begin{bmatrix} \frac{2(H-x_1)^{\beta+3} + (\beta+3)(H-x_1)H^{\beta+1}(\beta(H+x_1)+2x_1)}{2(\beta+1)(\beta+2)(\beta+3)} \\ \frac{2(H-x_2)^{\beta+3} + (\beta+3)(H-x_2)H^{\beta+1}(\beta(H+x_2)+2x_2)}{2(\beta+1)(\beta+2)(\beta+3)} \end{bmatrix} \quad (11)$$

Finally, the base moment of the central core under wind load and the presence of two outriggers is computed using Eq. (12), where $M_e$ represents the base moment.

$$M_e = \frac{wH^{\beta+2}}{\beta+2} - M_1 - M_2 \quad (12)$$

Moreover, the maximum lateral displacement at the top of the structure, considering the reduction in moment due to the outriggers, is calculated using the moment-area method and simplified into Eq. (13).

$$\Delta_o = \frac{w(2\beta+9)H^{\beta+4}}{6(\beta+3)(\beta+4)EI} - \frac{1}{2EI}(M_1(H^2 - x_1^2) + M_2(H^2 - x_2^2)) \quad (13)$$

### *2.2. Structure with (n) Outriggers*

After deriving the relations for a structure with two outriggers, these equations are generalized for a system with (n) outriggers. In this case, Eq. (11) is rewritten in its general form as Eq. (14).

$$\begin{bmatrix} M_1 & M_2 & \dots & M_i & \dots & M_n \end{bmatrix}^T = \frac{w}{EI} A^{-1} B$$

$$A = \begin{bmatrix} S_1 + S(H - x_1) & S(H - x_2) & \dots & S(H - x_n) \\ S(H - x_2) & S_1 + S(H - x_2) & \dots & S(H - x_n) \\ & & \vdots & \\ S(H - x_n) & S(H - x_n) & \dots & S_1 + S(H - x_n) \end{bmatrix}$$

$$B = \begin{bmatrix} \frac{2(H-x_1)^{\beta+3} + (\beta+3)(H-x_1)H^{\beta+1}(\beta(H+x_1)+2x_1)}{2(\beta+1)(\beta+2)(\beta+3)} \\ \frac{2(H-x_2)^{\beta+3} + (\beta+3)(H-x_2)H^{\beta+1}(\beta(H+x_2)+2x_2)}{2(\beta+1)(\beta+2)(\beta+3)} \\ \vdots \\ \frac{2(H-x_i)^{\beta+3} + (\beta+3)(H-x_i)H^{\beta+1}(\beta(H+x_i)+2x_i)}{2(\beta+1)(\beta+2)(\beta+3)} \\ \vdots \\ \frac{2(H-x_n)^{\beta+3} + (\beta+3)(H-x_n)H^{\beta+1}(\beta(H+x_n)+2x_n)}{2(\beta+1)(\beta+2)(\beta+3)} \end{bmatrix} \quad (14)$$

Accordingly, the base moment and maximum lateral displacement of the structure with (n) outriggers are computed from Eqs. (15) and (16).

$$M_e = \frac{wH^{\beta+2}}{\beta+2} - \sum_{i=1}^{n} M_i = \frac{wH^{\beta+2}}{\beta+2} - \frac{w}{EI} B^T (A^{-1})^T e^T \quad (15)$$

$$\Delta_o = \frac{w(2\beta+9)H^{\beta+4}}{6(\beta+3)(\beta+4)EI} - \frac{1}{2EI}\sum_{i=1}^{n} M_i(H^2 - x_i^2) = \frac{w(2\beta+9)H^{\beta+4}}{6(\beta+3)(\beta+4)EI} - \frac{1}{2EI}\frac{w}{EI} B^T (A^{-1})^T C \quad (16)$$

$$e = \begin{bmatrix} 1 & 1 & \dots & 1 \end{bmatrix}$$

$$C^T = \begin{bmatrix} H^2 - x_1^2 & H^2 - x_2^2 & \dots & H^2 - x_n^2 \end{bmatrix} \quad (17)$$

It should be noted that the present study is based on the equivalent static representation of wind loading, which is commonly adopted during the preliminary design of tall buildings. The parameter β is employed to characterize different vertical distributions of wind loading intensity and is not intended to represent the complete dynamic characteristics of wind excitation. Consequently, important aerodynamic phenomena such as vortex shedding, cross-wind vibrations, aerodynamic damping, and aeroelastic interactions are beyond the scope of the present analytical formulation. Although these effects may become significant for very slender or super-tall buildings, the proposed analytical model provides an efficient framework for evaluating the influence of wind load intensity on the optimal placement of outrigger systems under equivalent static loading. Future studies may extend the present formulation by incorporating dynamic wind loading models and aeroelastic effects.

## 3. Optimal Location of Outriggers for Minimizing Base Moment

According to Eq. (15), the base moment of the central core is a function of the outrigger locations x1, x2, x3,. … , xn. To determine the optimal outrigger placement that minimizes the base moment, Eq. (15) must be minimized. Considering that the first term of this equation is constant, minimizing the base moment is equivalent to maximizing the second term of the equation. To achieve this, the derivative of the second term with respect to each outrigger location x1, x2, x3, …, xn is taken, and the resulting system of (n) equations, corresponding to Eq. (18), is set to zero:

$$\begin{aligned} &\frac{\partial}{\partial x_1}\left(\frac{w}{EI} B^T (A^{-1})^T e^T\right) = 0 \\ &\frac{\partial}{\partial x_2}\left(\frac{w}{EI} B^T (A^{-1})^T e^T\right) = 0 \\ &\qquad\vdots \\ &\frac{\partial}{\partial x_i}\left(\frac{w}{EI} B^T (A^{-1})^T e^T\right) = 0 \\ &\qquad\vdots \\ &\frac{\partial}{\partial x_n}\left(\frac{w}{EI} B^T (A^{-1})^T e^T\right) = 0 \end{aligned} \quad (18)$$

Solving this system yields the optimal locations x1, x2, x3, …, xn that minimize the base moment of the structure.

To account for the influence of all structural components and to eliminate the dependence of the governing equations on absolute geometric and material properties, dimensionless parameters are defined as expressed in Eq. (19) [10].

$$\lambda = \frac{EI}{(EA)_C (\frac{d^2}{2})} \quad , \quad \gamma = \frac{EId}{(EI)_o H} \tag{19}$$

The parameter λ represents the stiffness ratio between the central core and the perimeter columns, while γ denotes the stiffness ratio between the central core and the outriggers. To incorporate the combined effects of all structural components on the optimal location of outriggers, a dimensionless parameter is defined by Eq. (20) [10].

$$\omega = \frac{\gamma}{12(1+\lambda)} \tag{20}$$

By introducing the parameter ω, the behavior of outrigger-supported structures can be described in a simplified and unified manner. For constant values of the other structural parameters, an increase in the flexural stiffness of the outriggers results in a decrease in ω, whereas an increase in the axial stiffness of the perimeter columns leads to an increase in this parameter. By solving the governing equations in terms of ω, the optimal outrigger locations that minimize the base moment of the structure can be determined.

Wind loading is influenced by several factors, including the geographical location of the building, ground roughness characteristics, and surface irregularities in the surrounding environment. In this study, to investigate the effect of wind intensity on the optimal location of outriggers, four different values of β (β=0.14, 0.26, 0.38,0.50) are considered. In addition, to evaluate the influence of the number of outriggers on the structural response, systems with 1, 2, 3, and 4 outriggers are examined.

### *3.1. Structure with One Outrigger*

Figures 3 and 4 illustrate the optimal outrigger location for a structure equipped with a single outrigger and the effect of wind intensity on its optimal location.

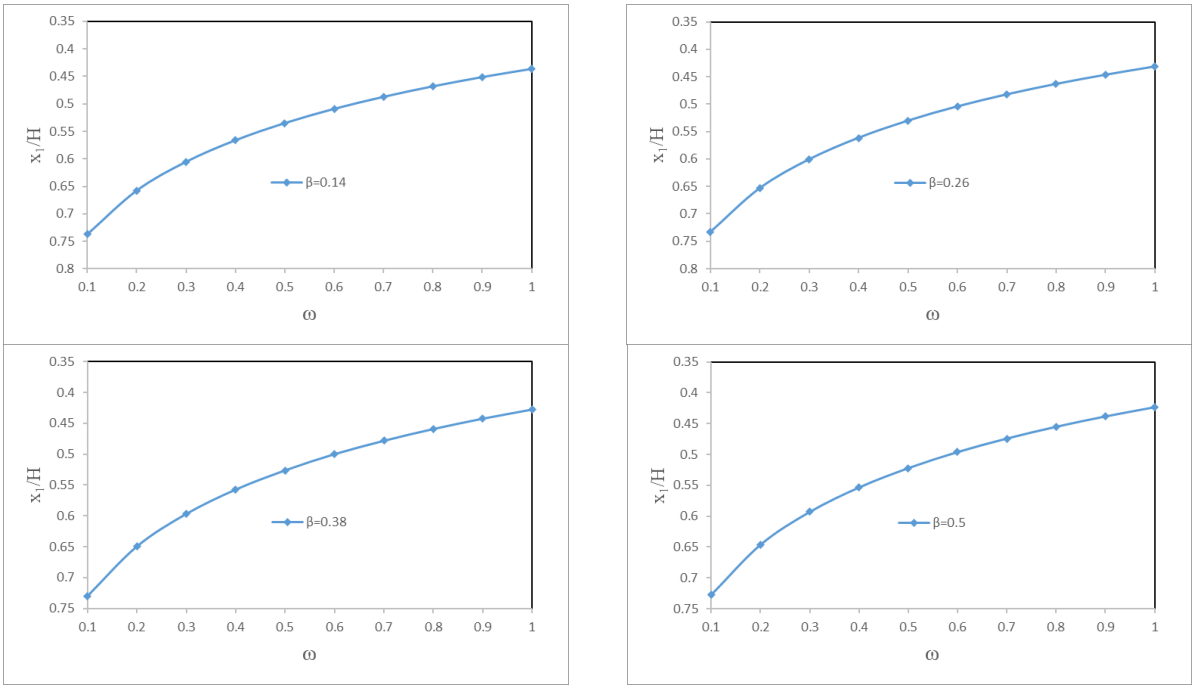


**Fig. 3:** Optimal outrigger location for a building with a single outrigger

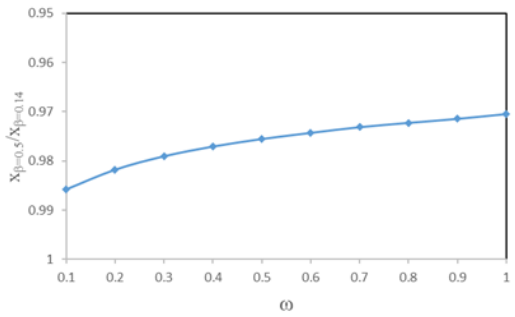


**Fig. 4:** Ratio of the optimum location of outrigger with intensity β=0.5 to intensity β=0.14

The results indicate that increasing the axial stiffness of the perimeter columns, increasing the flexural stiffness of the central core, and decreasing the flexural stiffness of the outrigger lead to a shift of the optimal outrigger location toward higher elevations of the building. Variations in the mechanical properties of the structural members can cause the optimal outrigger position to change by up to approximately 30% of the total building height. Furthermore, the influence of wind intensity on the optimal outrigger location is found to be relatively limited.

Nevertheless, as wind intensity increases, the optimal outrigger position corresponding to the minimization of the base moment tends to shift upward along the height of the structure.

### 3.2. Structure with Two Outriggers

Figures 5 and 6 present the optimal locations of the outriggers for a structure equipped with two outriggers, along with the influence of wind intensity on their optimal location.

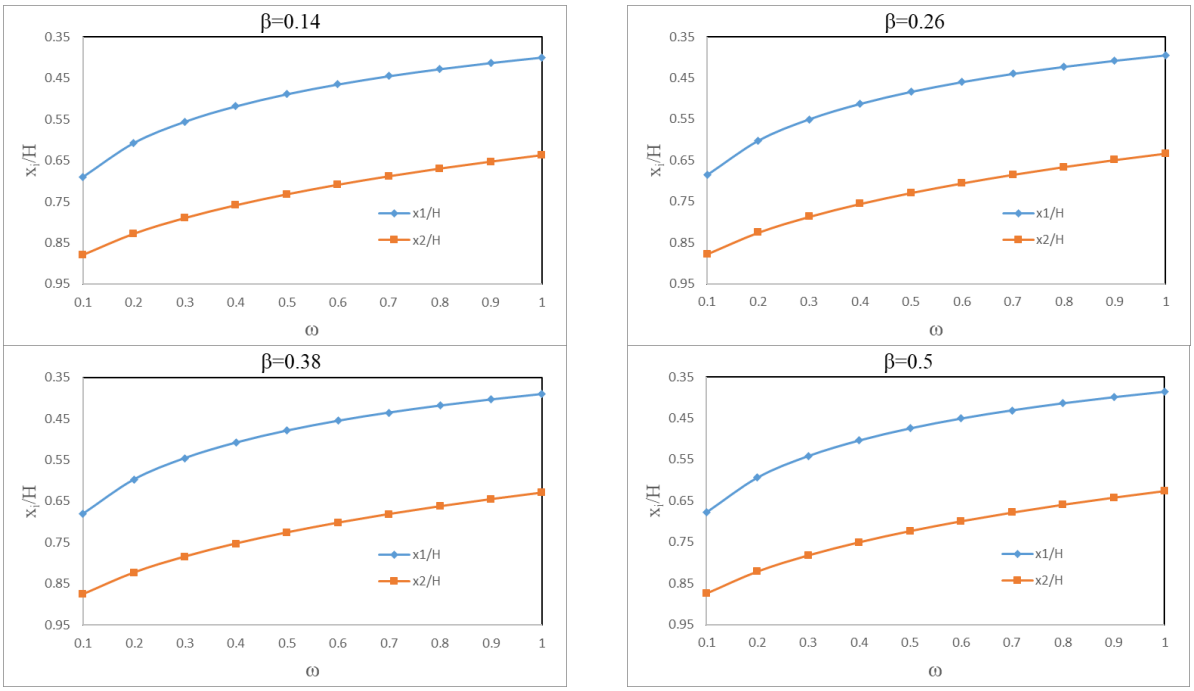


**Fig. 5:** Optimal outrigger location for a building with two outriggers

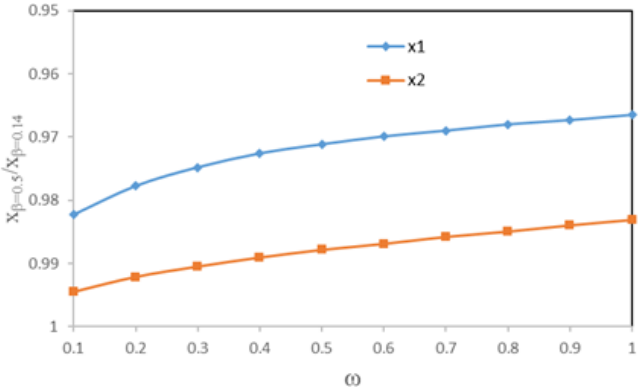


**Fig. 6:** Ratio of the optimum location of outriggers with intensity β=0.5 to intensity β=0.14

The results indicate that increasing the axial stiffness of the perimeter columns, increasing the flexural stiffness of the central core, or decreasing the flexural stiffness of the outriggers leads to an increase in the spacing between the two outriggers, while simultaneously shifting their locations toward higher elevations of the building.

Moreover, as wind intensity increases, the optimal spacing between the two outriggers becomes larger, and their optimal positions move upward along the height of the structure. It is also observed that when the ratio of the flexural stiffness of the central core to that of the outriggers is smaller, wind intensity has a more pronounced effect on the variation of the optimal outrigger locations, resulting in greater positional shifts.

### 3.3. Structure with Three Outriggers

Figures 7 and 8 illustrate the optimal outrigger locations for a structure equipped with three outriggers and the effect of wind intensity on their optimal location.

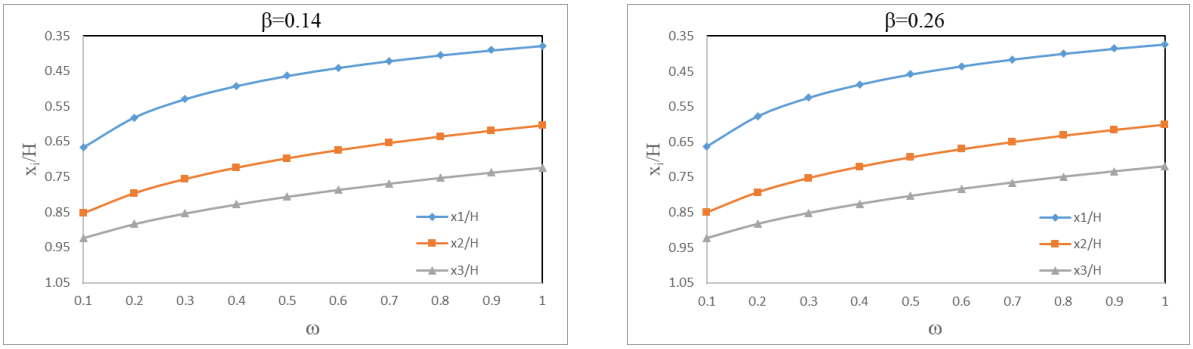

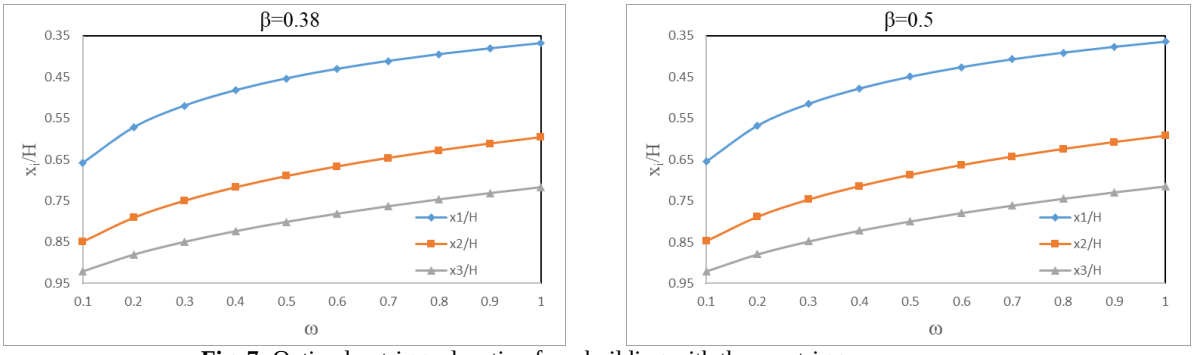


**Fig. 7:** Optimal outrigger location for a building with three outriggers

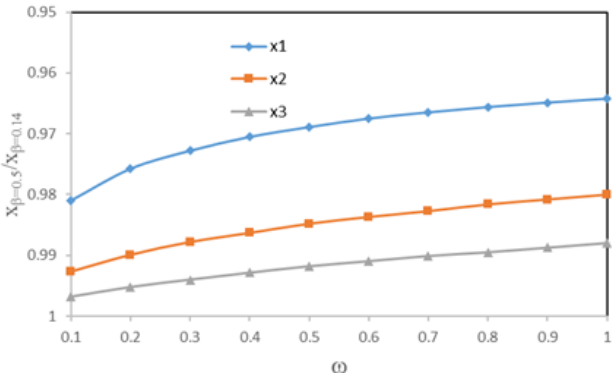


**Fig. 8:** Ratio of the optimum location of outriggers with intensity β=0.5 to intensity β=0.14

The results indicate that as the number of outriggers increases, those located at lower elevations tend to move closer to each other. In other words, in buildings with multiple outriggers, achieving the optimal configuration for minimizing the base moment may result in some outriggers being placed at adjacent or closely spaced levels. Furthermore, increasing the flexural stiffness of the outriggers leads to a reduction in the optimal spacing between them. With respect to wind intensity, the results reveal that as wind intensity increases, the outrigger located at higher elevations is more significantly affected, exhibiting a greater shift in its optimal position compared to the lower outriggers.

### *3.4. Structure with Four Outriggers*

Figures 9 and 10 illustrate the optimal outrigger locations for a structure equipped with four outriggers and the influence of wind intensity on their optimal location

.

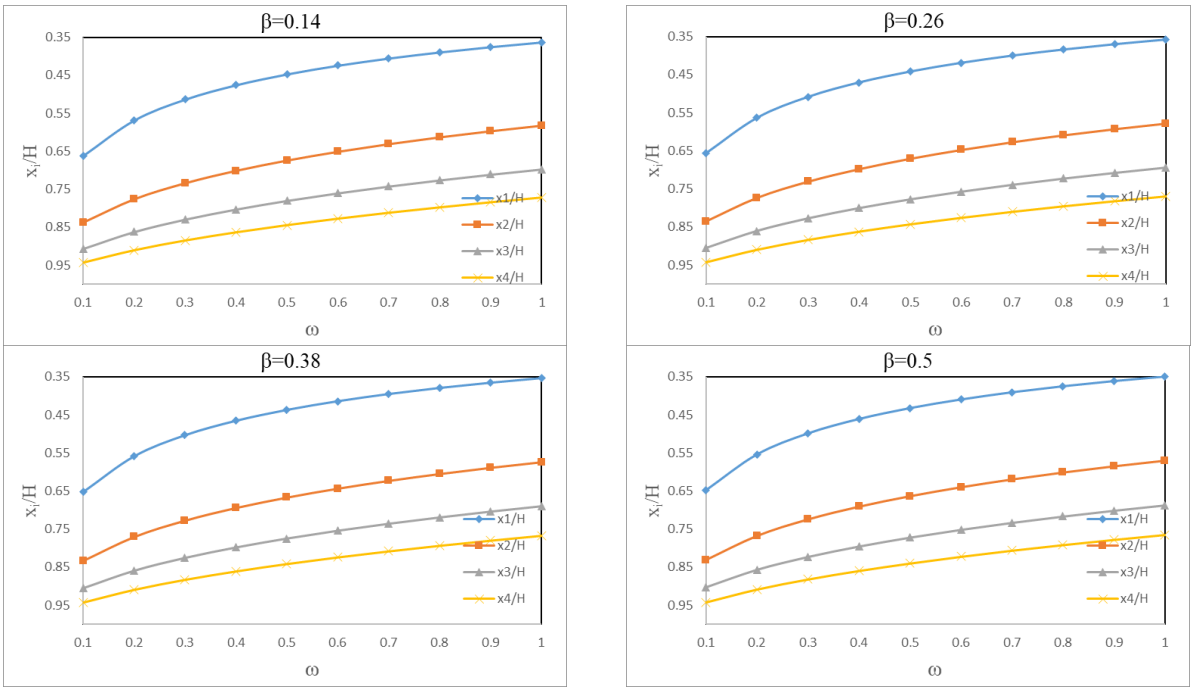


**Fig. 9:** Optimal outrigger location for a building with four outriggers

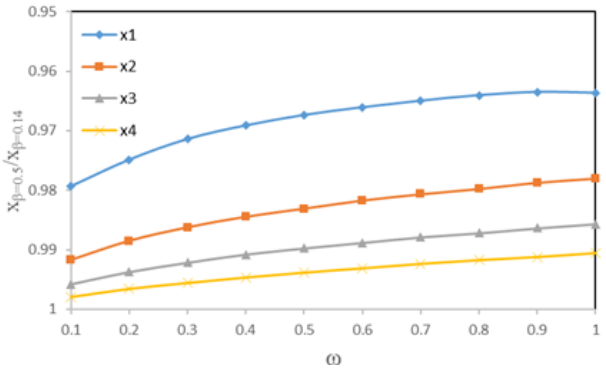


**Figure. 10.** Ratio of the optimum location of outriggers with intensity β=0.5 to intensity β=0.14

The results indicate that when the number of outriggers increases to four, and the ratio of the flexural stiffness of the outriggers to that of the central core is large, the outriggers tend to move closer to each other, potentially being located at adjacent floor levels. Moreover, when the flexural stiffness ratio between the outriggers and the central core becomes very large, increasing the number of outriggers does not lead to a significant improvement in structural performance in terms of reducing the base bending moment of the core. This behavior suggests that the outrigger system reaches a stiffness saturation state, beyond which adding more outriggers yields diminishing returns.

## 4. Optimal Outrigger Location for Minimizing Maximum Building Displacement

Using Eq. (16), the maximum lateral displacement of the building can be evaluated. To determine the optimal outrigger locations that minimize this displacement, Eq. (16) is differentiated with respect to the outrigger positions x1, x2, x3, …, xn. This procedure yields a system of n equations, which are set to zero according to Eq. (21).

$$\begin{aligned}
&\frac{\partial}{\partial x_1}\left(\frac{1}{2EI}\frac{w}{EI}B^T(A^{-1})^T C\right)=0\\
&\frac{\partial}{\partial x_2}\left(\frac{1}{2EI}\frac{w}{EI}B^T(A^{-1})^T C\right)=0\\
&\quad\vdots\\
&\frac{\partial}{\partial x_i}\left(\frac{1}{2EI}\frac{w}{EI}B^T(A^{-1})^T C\right)=0\\
&\quad\vdots\\
&\frac{\partial}{\partial x_n}\left(\frac{1}{2EI}\frac{w}{EI}B^T(A^{-1})^T C\right)=0
\end{aligned} \tag{21}$$

By simultaneously solving this system of equations, the optimal outrigger locations x1, x2, x3, …, xn that minimize the maximum lateral displacement of the building are obtained.

### *4.1. Structure with One Outrigger (Maximum Displacement Criterion)*

Figures 11 and 12 depict the optimal outrigger location and the influence of wind intensity on this location for a structure equipped with a single outrigger.

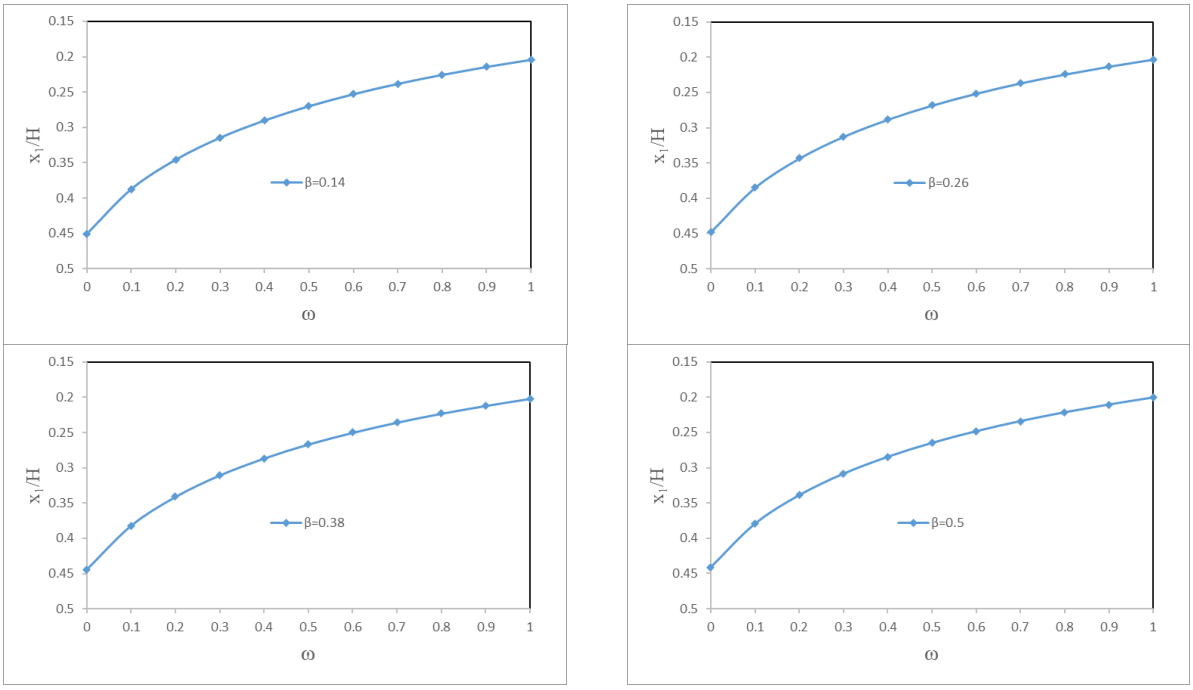


**Fig. 11:** Optimal outrigger location for a building with a single outrigger

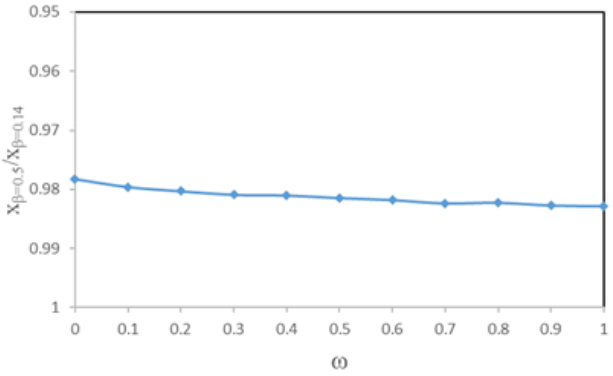


**Fig. 12:** Ratio of the optimum location of outriggers with intensity β=0.5 to intensity β=0.14

The results indicate that, in single-outrigger structures, wind intensity has a relatively minor effect on the displacement of the optimal outrigger position.

It is also observed that a reduction in the flexural stiffness of the central core or an increase in the flexural stiffness of the outrigger amplifies the effect of wind intensity on the optimal outrigger displacement. The flexural stiffness ratio between the central core and the outrigger exerts the most significant influence on the optimal outrigger location, whereas the axial stiffness of the columns has the least effect on the displacement of the outrigger position.

### *4.2. Structure with Two Outriggers (Maximum Displacement Criterion)*

Figure 13 illustrates the optimal outrigger locations for a structure with two outriggers subjected to wind loads of varying intensities. Figure 14 shows a comparison of the optimal outrigger locations for β=0.5 and β=0.14.

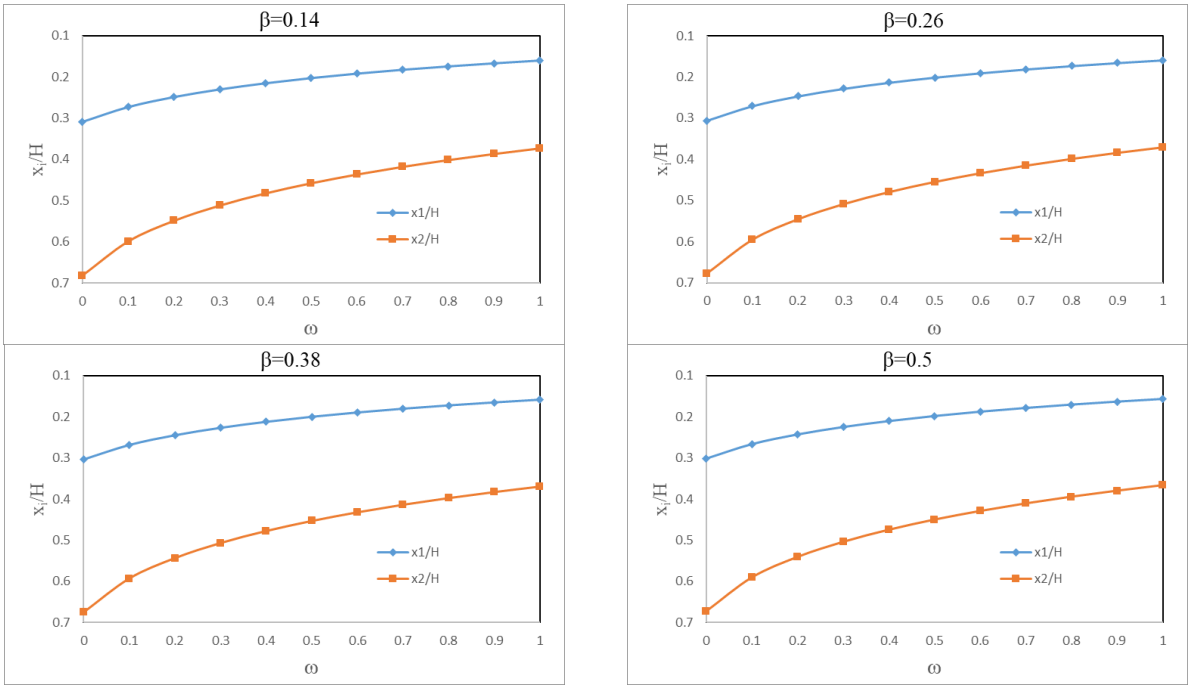


**Fig. 13:** Optimal outrigger location for a building with two outriggers

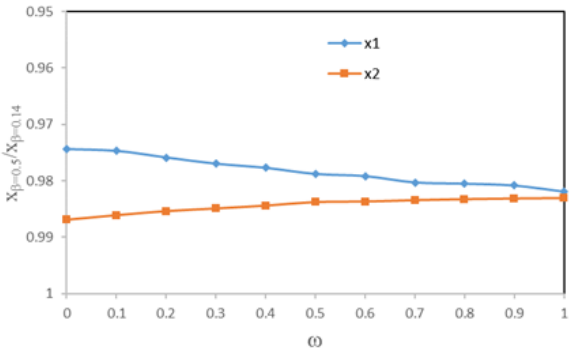


**Fig. 14:** Ratio of the optimum location of outriggers with intensity β=0.5 to intensity β=0.14

The results indicate that as wind intensity increases, and if the flexural stiffness ratio of the central core to the outriggers is large, the two outriggers move closer together, shifting the optimal outrigger locations toward the upper sections of the building. Conversely, as the axial stiffness of the columns decreases, the distance between the two outriggers increases, causing their optimal locations shift downward in the building. When the flexural stiffness of the outriggers is significantly higher than that of other structural components, the spacing between the outriggers increases, and their optimal location shifts downward in the structure.

### *4.3. Structure with Three Outriggers (Maximum Displacement Criterion)*

Figure 15 presents the optimal outrigger locations for a structure equipped with three outriggers subjected to wind loads of varying intensities. Figure 16 illustrates the ratios of the optimal outrigger locations corresponding to β=0.5 to those obtained for β=0.14.

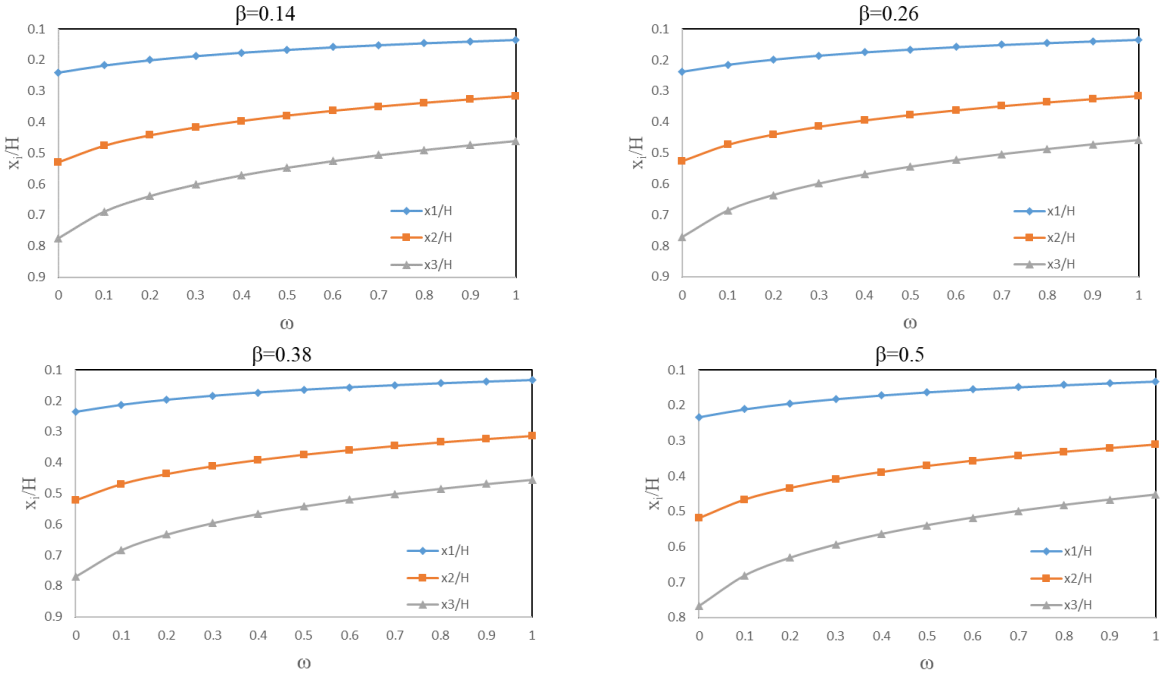


**Fig. 15:** Optimal outrigger location for a building with three outriggers

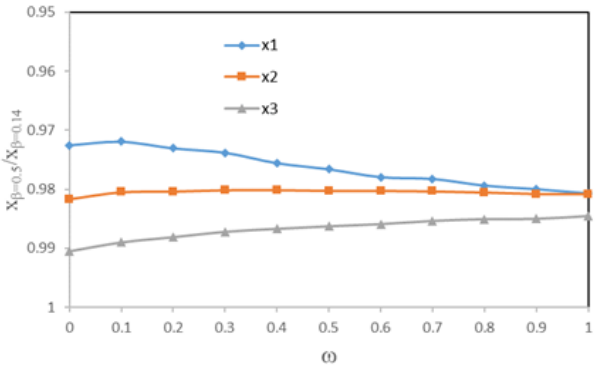


**Fig. 16:** Ratio of the optimum location of outriggers with intensity β=0.5 to intensity β=0.14

The results indicate that as the number of outriggers increases, those located at lower elevations of the building tend to move closer to each other compared to the outriggers placed at higher levels. In addition, increasing wind intensity causes the optimal outrigger locations to shift toward the upper portions of the building. It is also observed that increasing the flexural stiffness of the outriggers or decreasing the flexural stiffness of the central core amplifies the influence of wind intensity on the displacement of the optimal outrigger located at higher elevations.

### *4.4. Structure with Four Outriggers (Maximum Displacement Criterion)*

Figure 17 illustrates the optimal outrigger locations for a structure equipped with four outriggers subjected to wind loads of varying intensities. Figure 18 presents the ratios of the optimal outrigger locations corresponding to β=0.5 to those obtained for β=0.14.

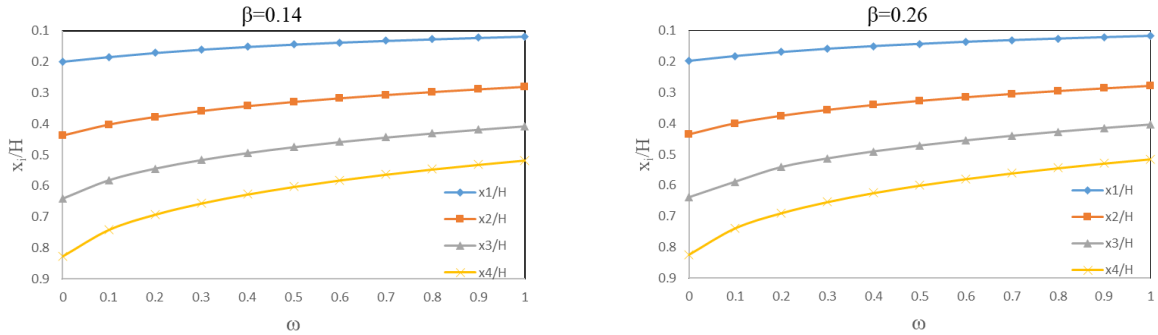

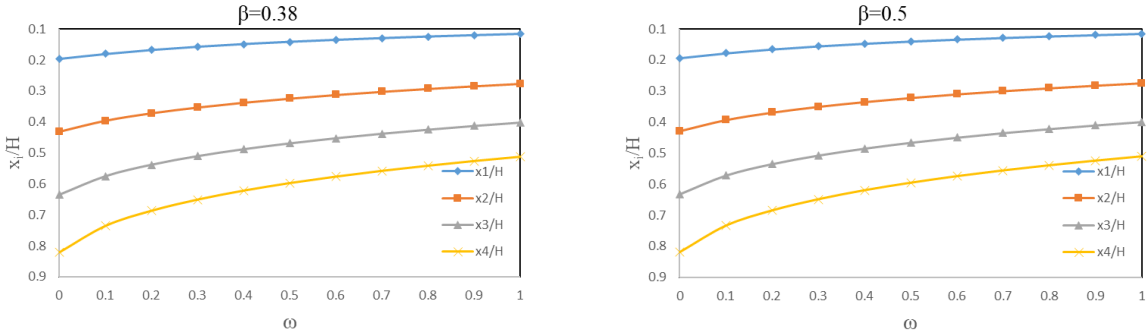


**Fig. 17:** Optimal outrigger location for a building with four outriggers

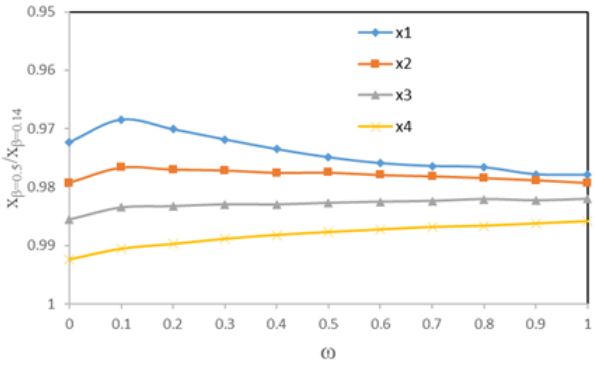


**Fig. 18:** Ratio of the optimum location of outriggers with intensity β=0.5 to intensity β=0.14

The results indicate that reducing the axial stiffness of the perimeter columns, while keeping the other structural parameters constant, amplifies the influence of wind intensity on the displacement of the optimal outrigger locations. Moreover, as the number of outriggers increases, the largest variation in the optimal location is observed for the lowest outrigger, whereas the smallest variation corresponds to the outrigger positioned at the highest elevation of the building.

## 5. Ratio of Optimal Outrigger Elevation for Minimizing Base Moment to That for Minimizing Maximum Displacement

Figures 19 to 22 present the ratio of the optimal outrigger elevations obtained for minimizing the base bending moment to those corresponding to minimizing the maximum building displacement, considering different numbers of outriggers.

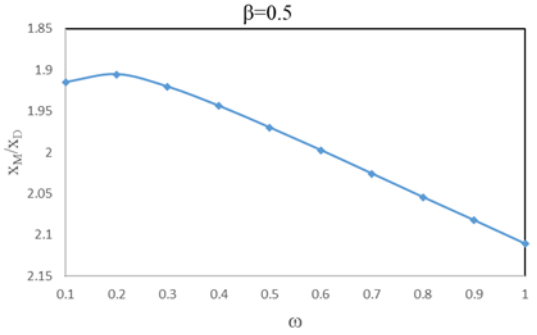


**Fig. 19:** Ratio of optimal location to minimize the base moment to minimize the maximum building displacement for one outrigger

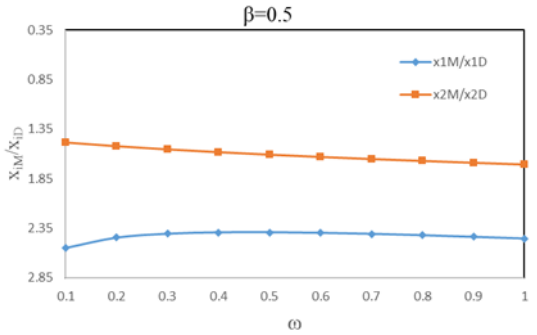


**Fig. 20:** Ratio of optimal location to minimize the base moment to minimize the maximum building displacement for two outriggers

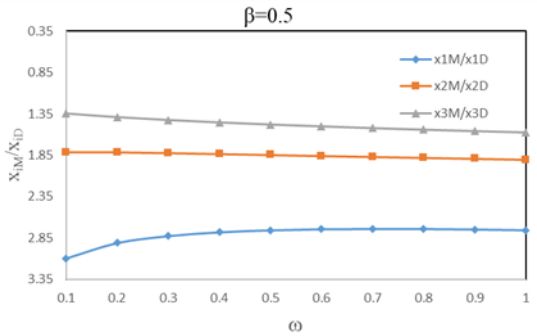


**Fig. 21:** Ratio of optimal location to minimize the base moment to minimize the maximum building displacement for three outriggers

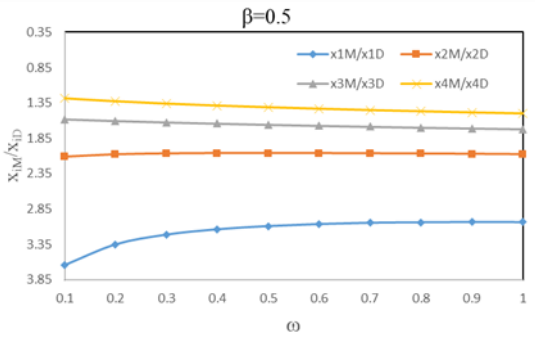


**Fig. 22:** Ratio of optimal location to minimize the base moment to minimize the maximum building displacement for four outriggers

The results demonstrate that the optimal outrigger locations derived based on the base moment minimization criterion are consistently positioned at lower elevations compared to those obtained from the maximum displacement minimization criterion. This difference reflects the fundamentally distinct nature of the two design objectives and their associated stiffness distribution requirements along the building height.

For structures equipped with a single outrigger, increasing the flexural stiffness of the central core or decreasing the flexural stiffness of the outrigger leads to a significant increase in the relative separation between the optimal locations corresponding to the two design criteria. This behavior highlights the high sensitivity of the optimal outrigger position to stiffness parameters in systems with a limited number of outriggers.

As the number of outriggers increases, the influence of variations in structural member properties on the ratio of optimal outrigger elevations for base moment and maximum displacement minimization becomes less pronounced, and the values of this ratio tend to converge. This indicates that employing multiple outriggers promotes a more unified structural response with respect to strength and serviceability performance criteria.

Although both optimization objectives are achieved by adjusting the outrigger locations, the governing structural mechanisms are fundamentally different. Minimizing the base moment is primarily associated with reducing the overturning moment transferred to the foundation through an efficient redistribution of internal forces between the core and the perimeter columns. In this case, the outrigger system acts mainly by mobilizing axial forces in the exterior columns, thereby reducing the bending moment carried by the core. Conversely, minimizing the maximum lateral displacement is governed by the global stiffness of the structural system. The outrigger location must therefore be selected to maximize the overall flexural stiffness and minimize the cumulative lateral deformation over the building height. Since one objective is controlled mainly by force redistribution whereas the other depends on deformation control, the corresponding optimal outrigger locations are generally different. This distinction becomes more evident as the wind loading intensity increases.

## 6. Discussion and Conclusion

In this study, the influence of wind load intensity on the optimal locations of outriggers for minimizing the maximum building displacement and the base bending moment of the central core was investigated. To this end, a set of simplifying assumptions was adopted to derive the governing analytical relationships in matrix form. The optimal outrigger locations under various wind intensities and different numbers of outriggers were determined using MATLAB. Based on the analysis of the obtained results, the following conclusions can be drawn:

The conducted parametric study also provides insight into the robustness of the proposed optimal outrigger locations. Since the parameters λ, γ, and ω represent the relative stiffness of the core, perimeter columns, and outrigger system, varying these parameters effectively evaluates the sensitivity of the analytical solution to changes in structural stiffness. The results indicate that the optimal outrigger locations vary gradually with changes in the stiffness ratio and wind loading intensity, while the overall optimization trends remain unchanged. This stable behavior suggests that the proposed analytical formulation is sufficiently robust for preliminary design applications. Consequently, selecting an intermediate location within the identified optimal region is expected to maintain satisfactory structural performance even under moderate variations in structural stiffness. Nevertheless, a formal robustness assessment based on quantitative sensitivity indices and multi-objective optimization techniques could provide further insight and is recommended for future studies.

The results indicate that increasing wind load intensity shifts the optimal outrigger locations toward higher elevations of the building while reducing the spacing between outriggers. This behavior reflects the dominant role of wind loading in activating the upper portions of tall buildings to control the overall structural response.

An increase in the flexural stiffness of the central core or a decrease in the flexural stiffness of the outriggers amplifies the sensitivity of the optimal outrigger locations to wind load intensity, leading to more pronounced shifts in their optimal positions as wind intensity varies.

Increasing the flexural stiffness of the central core, decreasing the flexural stiffness of the outriggers, or increasing the axial stiffness of the columns causes the optimal outrigger locations for both maximum displacement minimization and base moment

minimization to move upward along the building height, while simultaneously reducing the spacing between outriggers. This observation highlights the strong interaction between stiffness distribution and lateral load transfer mechanisms in outrigger-supported systems.

A comparative evaluation of the two design criteria reveals a significant discrepancy between the optimal outrigger locations obtained for minimizing the base bending moment of the central core and those corresponding to minimizing the maximum building displacement, particularly in structures with a limited number of outriggers. This finding emphasizes the importance of explicitly selecting the governing design objective during the preliminary design stages of tall buildings.

The proposed analytical formulation is intended as a preliminary design and analytical tool for evaluating the influence of wind loading intensity on the optimal placement of outrigger systems. Although the governing equations are derived from established structural mechanics principles, further validation using detailed finite element models, such as ETABS, SAP2000, or Abaqus, would provide additional confidence in the applicability of the proposed approach to practical structural design. Such validation constitutes an important direction for future research.

From a practical design perspective, the proposed analytical relationships provide structural engineers with an efficient tool for estimating the influence of wind loading intensity on the optimal placement of outrigger systems during the preliminary design stage. The results demonstrate that variations in wind load intensity and structural stiffness can significantly alter the optimal outrigger configuration depending on the selected structural performance criterion. Consequently, these parameters should be carefully considered during the conceptual design of high-rise buildings.

The present analytical formulation is based on several simplifying assumptions, including linear elastic structural behavior, equivalent static wind loading, constant structural stiffness along the building height, and the neglect of shear lag and second-order (P–Δ) effects. These assumptions enable the derivation of closed-form analytical relationships but may limit the direct applicability of the model to complex structural systems exhibiting significant nonlinear or dynamic behavior. Future research may focus on extending the proposed analytical framework by incorporating geometric nonlinearity, variable stiffness distributions along the building height, shear lag effects, and dynamic wind loading.

## References

**[1]** Hasançebi, O., Bahçecioglu, T., Kurç, O., & Saka, M. P. (2011). Optimum design of high-rise steel buildings using an evolution strategy integrated parallel algorithm. Computers & Structures, 89 (21–22), 2037–2051. https://doi.org/10.1016/j.compstruc.2011.05.019

**[2]** Zhang, Z. H., & Li, Q. S. (2023). Seismic responses of super high-rise buildings under long-period ground motions. Engineering Structures, 294, 116824. https://doi.org/10.1016/j.engstruct.2023.116824

**[3]** Wen, Z., Bai, K., Hong, H., et al. (2023). Development of locally resonant metabasement for seismic-induced vibration control of high-rise buildings. Engineering Structures, 275, 115229. https://doi.org/10.1016/j.engstruct.2022.115229

**[4]** Zhou, K., & Li, Q. S. (2022). Vibration mitigation performance of active tuned mass damper in a super high-rise building during multiple tropical storms. Engineering Structures, 269, 114840. https://doi.org/10.1016/j.engstruct.2022.114840

**[5]** Alhaddad, W., Halabi, Y., Xu, H., & Lei, H. (2020). A comprehensive introduction to outrigger and belt-truss system in skyscrapers. Structures, 27, 989–998. https://doi.org/10.1016/j.istruc.2020.06.028

**[6]** Bhandari, M., Bharti, S. D., Shrimali, M. K., & Datta, T. K. (2021). Applicability of capacity spectrum method for base-isolated building frames at different performance points. Journal of Earthquake Engineering, 25(2), 270–299. https://doi.org/10.1080/13632469.2019.1582190

**[7]** Bozorgnia, Y., Niazi, M., & Campbell, K. W. (1995). Characteristics of free-field vertical ground motion during the Northridge earthquake. Earthquake Spectra, 11(4), 515–525. https://doi.org/10.1193/1.1585828

**[8]** Shehzad, A., Yosri, A. M., Wang, X.-X., Akbar, M., Alzara, M., Siddiqui, N. A., Kashif, M., & Zaghloul, Y. (2025). A systematic review on seismic resilience in high-rise structures to enhance outrigger systems. Structures, 82, 110753. https://doi.org/10.1016/j.istruc.2025.110753

**[9]** Zhou, Y., Zhang, C. Q., & Lu, X. L. (2016). An inter-story drift-based parameter analysis of the optimal location of outriggers in tall buildings. The Structural Design of Tall and Special Buildings, 25(5), 215–231. https://doi.org/10.1002/tal.1260

**[10]** Smith, B. S., & Coull, A. (1991). Tall building structures: Analysis and design. John Wiley & Sons.

**[11]** Malekinejad, M., & Rahgozar, R. (2011). Free vibration analysis of tall buildings with outrigger–belt truss system. Earthquake and Structures, 2(1), 89–107. https://doi.org/10.12989/eas.2011.2.1.089

**[12]** Wu, J., & Li, Q. S. (2003). Structural performance of multi-outrigger-braced tall buildings. The Structural

Design of Tall and Special Buildings, 12(2), 155–176. https://doi.org/10.1002/tal.222

**[13]** Zhang, Z., Fu, X., Wang, J., & Wei, Y. (1996). Studies on structural performance of ultra-high-rise buildings with outrigger belts. Journal of Building Structures, 17(2), 2–9.

**[14]** Xing, L., Gardoni, P., Zhou, Y., & Zhang, P. (2023). Optimal models of outrigger locations and damping parameter for combined energy dissipation outrigger systems subject to seismic and wind loads. Journal of Building Engineering, 76, 107209. https://doi.org/10.1016/j.jobe.2023.107209

**[15]** Kim, H.-S., Lim, Y.-J., & Lee, H.-L. (2020). Optimum location of outrigger in tall buildings using finite element analysis and gradient-based optimization method. Journal of Building Engineering, 31, 101379. https://doi.org/10.1016/j.jobe.2020.101379

**[16]** Chen, Y., & Zhang, Z. (2018). Analysis of outrigger numbers and locations in outrigger-braced structures using a multi-objective genetic algorithm. The Structural Design of Tall and Special Buildings, 27(1), e1408. https://doi.org/10.1002/tal.1408

**[17]** Lee, S. B., & Tovar, A. (2014). Outrigger placement in tall buildings using topology optimization. Engineering Structures, 74, 122–129. https://doi.org/10.1016/j.engstruct.2014.05.010

**[18]** Kamgar, R., & Rahgozar, R. (2017). Determination of optimum location for flexible outrigger systems in tall buildings with constant cross section using energy method. International Journal of Steel Structures, 17(1), 1–8. https://doi.org/10.1007/s13296-016-9017-5

**[19]** Hoenderkamp, J. C. D. (2008). Second outrigger at optimum location on high-rise shear wall. The Structural Design of Tall and Special Buildings, 17(3), 619–634. https://doi.org/10.1002/tal.395

**[20]** WU, J., & LI, Q. S. (2003). STRUCTURAL PERFORMANCE OF MULTI-OUTRIGGERBRACED TALL BUILDINGS. Struct. Design Tall Spec. Build, 12, 155–176. https://doi.org/10.1002/tal.219

**[21]** Afshar, M. A., Taherkhani, A. H., Khanlari, B. (2025). Study on performance of various installation makeups of damped outrigger systems. Advances in Structural Engineering, 29. https://doi.org/10.1177/13694332251391468

This article is an open-access article distributed under the terms and conditions of the Creative Commons Attribution (CC-BY) license.